TOXICOLOGICAL SCIENCES **107(1)**, 171–181 (2009)
doi:10.1093/toxsci/kfn226
Advance Access publication November 7, 2008

Synaptosomal Toxicity and Nucleophilic Targets of 4-Hydroxy-2-Nonenal

Richard M. LoPachin,*,[1] Brian C. Geohagen,* and Terrence Gavin†

*Department of Anesthesiology, Albert Einstein College of Medicine, Montefiore Medical Center, Bronx, New York 10467; and †Department of Chemistry, Iona College, New Rochelle, New York 10804

Received October 2, 2008; accepted October 15, 2008

4-Hydroxy-2-nonenal (HNE) is an aldehyde by-product of lipid peroxidation that is presumed to play a primary role in certain neuropathogenic states (e.g., Alzheimer disease, spinal cord trauma). Although the molecular mechanism of neurotoxicity is unknown, proteomic analyses (e.g., tandem mass spectrometry) have demonstrated that this soft electrophile preferentially forms Michael-type adducts with cysteine sulfhydryl groups. In this study, we characterized HNE synaptosomal toxicity and evaluated the role of putative nucleophilic amino acid targets. Results show that HNE exposure of striatal synaptosomes inhibited ^{3}H-dopamine membrane transport and vesicular storage. These concentration-dependent effects corresponded to parallel decreases in synaptosomal sulfhydryl content. Calculations of quantum mechanical parameters (softness, electrophilicity) that describe the interactions of an electrophile with its nucleophilic target indicated that the relative softness of HNE was directly related to both the second-order rate constant (k_2) for sulfhydryl adduct formation and corresponding neurotoxic potency (IC_{50}). Computation of additional quantum mechanical parameters that reflect the relative propensity of a nucleophile to interact with a given electrophile (chemical potential, nucleophilicity) indicated that the sulfhydryl thiolate state was the HNE target. In support of this, we showed that the rate of adduct formation was related to pH and that N-acetyl-L-cysteine, but not N-acetyl-L-lysine or β-alanyl-L-histidine, reduced *in vitro* HNE neurotoxicity. These data suggest that, like other type 2 alkenes, HNE produces nerve terminal toxicity by forming adducts with sulfhydryl thiolates on proteins involved in neurotransmission.

Key Words: **α,β-unsaturated carbonyl; nerve terminal toxicity; Alzheimer disease; acrolein; oxidative stress.**

4-Hydroxy-2-nonenal (HNE) is a reactive aldehyde by-product generated during peroxidation of membrane-derived ω6 polyunsaturated fatty acids such as arachidonic and linoleic acids (Montine *et al.*, 2002; Sayre *et al.*, 2001; Uchida, 2003). Lipid peroxidation occurs secondary to neuronal oxidative stress, which appears to be an initiating pathogenic event in central nervous system trauma (e.g., spinal cord injury) and certain neurodegenerative states (e.g., Alzheimer disease [AD], Parkinson disease; Halliwell, 2006; Jenner, 2003; Mattson, 2004). Indeed, it has been suggested that the neurotoxic consequences of oxidative stress are mediated by HNE and another reactive aldehyde by-product of membrane peroxidation, acrolein (Lovell *et al.*, 2000, 2001; Uchida, 2003; Zarkovic, 2003). Although the molecular mechanism of aldehyde neurotoxicity has not been adequately defined, HNE and acrolein are members of a diverse chemical family, the type 2 alkenes (Fig. 1). Chemicals in this family, which includes other well-known neurotoxicants, for example, acrylamide (ACR), acrylonitrile (LoPachin *et al.*, 2007a), are characterized by a conjugated structure formed when an electrophilic group (e.g., carbonyl) is linked to an alkene carbon (Kemp and Vellaccio, 1980). Because the *pi* electrons of a conjugated system are highly polarizable (mobile), the α,β-unsaturated carbonyl structure of HNE and other type 2 alkenes is a soft electrophile. Soft electrophiles preferentially form Michael-type adducts with soft nucleophiles, which in biological systems are primarily sulfhydryl groups on cysteine residues (Hinson and Roberts, 1992; LoPachin and DeCaprio, 2005). Indeed, recent kiinetic analyses (e.g., Doorn and Petersen, 2002, 2003; LoPachin *et al.*, 2007b) and proteomic determinations (e.g., Aldini *et al.*, 2005; Barber and LoPachin, 2004; Doorn and Petersen, 2003; van Iersel *et al.*, 1997) have confirmed the targeting of cysteine residues by HNE and other type 2 alkenes preferentially form adducts with sulfhydryl groups on cysteine residues. That these adducts have toxicological significance is evidenced by the fact that many neuronal processes (e.g., neurotransmitter release) involve proteins (e.g., N-ethylmaleimide-sensitive factor [NSF]) that are regulated by the redox state of specific cysteine sulfhydryl groups (Lipton *et al.*, 2002; LoPachin and Barber, 2006; LoPachin *et al.*, 2008a).

The reaction of a soft electrophile with a soft nucleophile is governed by the shape and energy of the respective frontier molecular orbitals (Chattaraj, 2001). Therefore, the ability of HNE to form adducts with cysteine sulfhydryl groups can be defined by quantum mechanical parameters such as softness (σ) and chemical potential (μ) (Chattaraj *et al.*, 2006; Pearson, 1990). These molecular descriptors have been used in earlier

[1] To whom correspondence should be addressed at Montefiore Medical Center, Moses Research Tower-7, 111 East 210th Street, Bronx, NY 10467. Fax: (718) 515-4903. E-mail: lopachin@aecom.yu.edu.

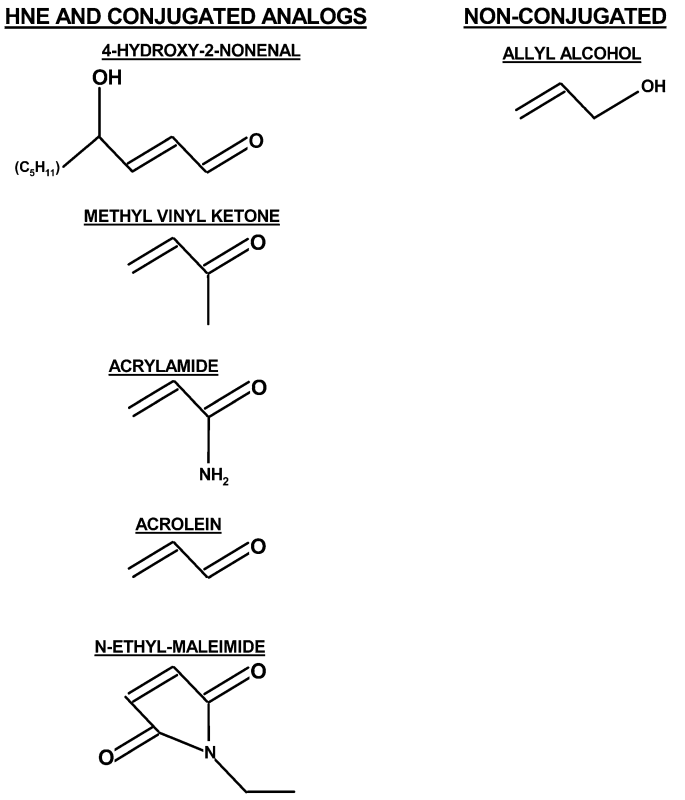

FIG. 1. This figure presents the line structures for HNE and several structurally related α,β-unsaturated carbonyl derivatives of the type 2 alkene class. Also shown is the line structure for the nonconjugated structural analog, allyl alcohol.

structure-toxicity studies of α,β-unsaturated derivatives to identify mechanisms of toxicity (LoPachin *et al*., 2007b; Maynard *et al*., 1998; Shultz *et al*., 2005). Furthermore, calculations of these parameters and kinetic analyses of the sulfhydryl adduct reactions have indicated that the anionic thiolate state of cysteine residues is the preferred target of type 2 alkenes (LoPachin *et al*., 2007b). Our previous research focused on small (3–6 carbon), water-soluble type 2 alkenes that are recognized environmental contaminants (e.g., acrolein, methyl vinyl ketone [MVK], methyl acrylate). In contrast, HNE is an endogenous product of cellular oxidative stress. Additionally, steric hindrance imparted by the alkane tail of this α,β-unsaturated carbonyl derivative (Fig. 1) could modify the kinetics of adduct formation and, hence, corresponding neurotoxic potency (Friedman and Wall, 1966). Therefore, in the present study, we determined the effects (IC_{50}'s) of HNE on brain synaptosomal function and defined the relative neurotoxic potency within the type 2 alkene chemical class. In addition, several quantum mechanical parameters of electrophilicity (e.g., softness, electrophilic index) were computed for HNE and selected conjugated alkenes. Values were compared to corresponding second-order rate constants (k_2) and neurotoxic potencies. Our results extend related synaptosomal research (e.g., Keller *et al*., 1997a,b) and suggest that HNE, like other type 2 alkenes, causes nerve terminal damage by forming adducts with sulfhydryl thiolate groups on proteins that play critical roles in neurotransmission.

MATERIALS AND METHODS

Chemicals and materials. Unless otherwise indicated, all reagents were high-performance liquid chromatography grade or better, and water was doubly distilled and deionized. ACR, acrolein, MVK, β-alanyl-L-histidine (carnosine), N-acetyl-L-cysteine (NAC), N-acetyl-L-lysine (NAL), Krebs-Henseleit buffer, and Percoll were purchased from the Sigma/Aldrich Chemical Company (Bellefonte, PA). HNE was purchased from Cayman Chemical Co. (Ann Arbor, MI) and was supplied in ethanol and stored at − 80°C. Aliquots of HNE were evaporated with nitrogen gas and reconstituted in Krebs-N-[2-hydroxyethyl]-piperazine-N'-[2-ethanesulfonic acid] (HEPES) buffer. The concentration of HNE was determined by UV absorbance at 224 nm with a molar absorptivity of 13,750/M. ^{3}H-Dopamine (^{3}H-DA; specific activity 23.5 Ci/mmol) was obtained from American Radiolabeled Chemicals (St Louis, MO). Whatman GF/F filter paper and Whatman GF/B filter disc were purchased from the Brandel Company (Gaithersburg, MD).

Animals. All aspects of this study were in accordance with the National Institutes of Health Guide for Care and Use of Laboratory Animals and were approved by the Montefiore Medical Center Animal Care Committee. Adult male rats (Sprague-Dawley, 300–325 g; Taconic Farms, Germantown, NY) were used in this study. Rats were housed individually in polycarbonate boxes, and drinking water and Purina Rodent Laboratory Chow (Purina Mills, Inc., St Louis, MO) were available *ad libitum*. The animal room was maintained at approximately 22°C and 50% humidity with a 12-h light/dark cycle.

Preparation of striatal synaptosomes and synaptic vesicles. Rat brain striatal synaptosomes were isolated by the Percoll gradient method of LoPachin *et al*. (2004). In brief, bilateral striata (100–120 mg wet weight tissue) were rapidly removed from anesthetized (isoflurane inhalation) rats and minced in cold (4°C) sucrose gradient buffer (pH 7.4). Tissue was gently homogenized in buffer (10 passes in a Teflon-glass homogenizer; 700 revolutions per minute), and the resulting homogenate was centrifuged at 1000 × g (10 min, 4°C). The pellet (P1) was washed once, and supernatants (S1 and S2) were combined. The supernatant was layered on top of a freshly prepared four-step discontinuous Percoll gradient (3, 10, 15, and 23% Percoll in sucrose buffer, pH 7.4). Gradients were centrifuged at 32,000 × g for 6 min, and synaptosomes were collected at the last interface (15%/23%). Synaptosomes were washed twice in Kreb's buffer (pH 7.4), pelleted, and then resuspended.

Striatal synaptic vesicles were prepared according to LoPachin *et al*. (2006). In brief, rat striata were homogenized in ice-cold 0.32M sucrose in a glass homogenizer using 10 strokes of a Teflon pestle. The homogenate was centrifuged at 800 × g for 12 min, and the resulting supernatant was centrifuged at 22,000 × g for 10 min. The P2 crude synaptosomal pellet was subjected to osmotic shock (5 min) by homogenization (five strokes with Teflon pestle) in 2 ml of distilled water. Osmolarity was restored by addition (1 ml) of a HEPES (0.25M)-potassium tartrate (1M) buffer (pH 7.5). The suspension was centrifuged at 20,000 × g for 20 min, and the supernatant was centrifuged at 55,000 × g for 60 min. $MgSO_4$ (1mM) buffer was added to the supernatant, which was then centrifuged at 100,000 × g for 50 min. The P5 pellet, which contained the isolated synaptic vesicles (20–30 μg protein), was resuspended in vesicle assay buffer.

In Vitro *Effects of HNE on Synaptosomal and Vesicular Function*

Synaptosomal membrane transport. Striatal synaptosomes (10 μg protein) were incubated with graded concentrations of HNE or Krebs-HEPES buffer for 15 min at 30°C (LoPachin *et al*., 2004). Synaptosomes were then washed, filter trapped by rapid filtration through a cell harvester (see above), and superfused (3 min) with Krebs-HEPES buffer containing ^{3}H-DA (0.30μM).

To correct for low-affinity Na^+-independent transport, uptake was measured in the presence and absence (equimolar choline chloride substitution) of sodium ions. Synaptosomes were then washed, and corresponding radioactivity was measured by scintillation counting. The concentration-response data for transport were fitted by nonlinear regression analysis, and the concentration producing 50% inhibition (IC_{50}′s with 95% confidence intervals) was calculated by the Cheng-Prusoff equation (Prism; GraphPad Software, San Diego, CA). To investigate nucleophilicity as a determinant of type 2 alkene amino acid targets, synaptosomes were preincubated (1 min) with either NAC (500μM), carnosine (500μM), or NAL (500μM) and then exposed (15 min) to graded concentrations of HNE, acrolein, MVK, or ACR. Synaptosomal uptake of ^{3}H-DA was determined as described above. The concentration-response data for transport were fitted by nonlinear regression analysis, and the IC_{50}′s (95% confidence intervals) were calculated by the Cheng-Prusoff equation (Prism; GraphPad Software).

Vesicular transport. Synaptic vesicles (3 μg protein) were exposed (15 min) to graded concentrations of HNE or control assay buffer. Vesicles were then incubated in assay buffer (200 μl) containing Mg^{2+}-adenosine triphosphate (ATP) (2mM) and 0.30μM ^{3}H-DA for 3 min at 30°C (LoPachin *et al*., 2006). The uptake reaction was terminated by addition of cold assay buffer (1 ml), and vesicles were collected onto Whatman GF/F glass fiber filters by rapid filtration through a Brandel cell harvester. Nonspecific uptake was determined by measuring vesicular ^{3}H-DA transport at 4°C in the absence of Mg^{2+}-ATP. Filters were washed, and trapped radioactivity was counted by scintillation spectroscopy. To determine the IC_{50} for HNE, the concentration-response data for vesicular transport were fitted by nonlinear regression analysis (r^2 for all curves > 0.90). IC_{50}′s and respective 95% confidence intervals were calculated by the Cheng-Prusoff equation (Prism; GraphPad Software).

Kinetic analysis of HNE neurotoxicity: synaptosomal and vesicular transport. In separate studies, we determined the effects of *in vitro* HNE on the kinetic parameters of DA transport in striatal synaptosomes and synaptic vesicles (for methodological details, see LoPachin *et al*., 2004, 2006, 2007a). Briefly, synaptosomes (10 μg protein) were exposed (15 min × 30°C) to the corresponding IC_{50} of HNE (450 μm) or to Krebs-HEPES buffer. HNE-exposed and control synaptosomes were washed, filter trapped, and superfused with graded ^{3}H-DA concentrations (50nM–1.7μM). To measure the effects of HNE on the kinetics of vesicular transport, synaptic vesicles (3 μg protein) were preexposed (15 min × 30°C) to the corresponding IC_{50} (60μM) and then incubated (3 min) with the graded ^{3}H-DA concentrations (50nM–1.7μM). For these studies, kinetic parameters (K_m, V_{max}) were determined by nonlinear regression analysis (Prism; GraphPad Software). Respective kinetic data for the control and experimental groups were compared statistically ($P < 0.05$) by a two-tailed Student *t*-test (InStat; GraphPad Software).

Measurement of free sulfhydryl groups. The concentration-dependent effects of HNE analogs on total free sulfhydryl content in synaptosomes were determined by the method of LoPachin *et al.* (2004). Following incubation (15 min) with graded concentrations of HNE or control buffer solutions, synaptosomes (200 μg protein) were solubilized with 1% SDS. 5,5′-Dithiobis(2-nitrobenzoic acid) (DTNB; 3mM) was added, and following equilibration (5 min, 25°C), absorbance was read at 412 nm using a Jenway 6305 spectrophotometer. A reagent blank without DTNB was used to zero the spectrophotometer. The concentration of 3-carboxylato-4-nitrothiophenolate, the thiol anion released during adduction of sulfhydryl groups by the disulfide reagent DTNB, was calculated by the molar extinction coefficient, 1.36×10^4/M/cm. The free sulfhydryl data for HNE were fitted by nonlinear regression analysis (r^2 for all curves ≥ 0.90), and respective IC_{50}′s and 95% confidence intervals were calculated by the Cheng-Prusoff equation (Prism 3.0; GraphPad Software).

Quantum mechanical parameters: LUMO, HOMO, η, μ, σ, ω, and ω⁻. The lowest unoccupied molecular orbital (LUMO) energy (E_{LUMO}) and highest occupied molecular orbital (HOMO) energy (E_{HOMO}), were calculated using Spartan04 (version 1.0.3) software (Wavefunction, Inc., Irvine, CA). Single-point energies for each structure were calculated at the density functional level of theory using a B3LYP-6-31G* basis set from 6-31G* geometries. Global (whole molecule) hardness (η) was calculated as $\eta = (E_{LUMO} - E_{HOMO})/2$, and chemical potential (μ) was calculated as $\mu = (E_{LUMO} + E_{HOMO})/2$ (Chattaraj *et al*., 2006). Softness (σ) is used as defined in Pearson (1990) and Maynard *et al*. (1998) and is calculated as the inverse of hardness or $\sigma = 1/\eta$. The electrophilicity index (ω) was calculated as $\omega = \mu^2/2\eta$ (Chattaraj *et al*., 2006), and the nucleophilicity index (ω^-) as $\omega^- = \eta_A (\mu_A - \mu_B)^2/2(\eta_A - \eta_B)^2$, where A = reacting nucleophile and B = reacting electrophile (Jaramillo *et al*., 2006). Linear regression analysis was used to assess the relationship between the calculated quantum mechanical parameters and neurotoxic potency (IC_{50}′s; Table 1) or kinetic data (k, k_2; Tables 1 and 3). Corresponding coefficients of determination (r^2) were calculated from the Pearson correlation coefficient (InStat 3.0; GraphPad Software) and are provided in the text.

TABLE 1
Kinetic Analysis of HNE Inhibition of Synaptosomal and Vesicular Transport

	Control		Acrolein		HNE	
Transport	V_{max}	K_m	V_{max}	K_m	V_{max}	K_m
Synaptosomal	34	270	18*	303	21*	336
Vesicular	42	310	26*	459*	22*	391

Note. The V_{max} is expressed as nmol/mg/min (synaptosomal) or fmol/μg/min (vesicular). The K_m is presented as nanomolar dopamine. Kinetic parameters (K_m, V_{max}) were determined by nonlinear regression analysis. Respective kinetic data for the control and experimental groups were compared statistically ($P < 0.05$) by a two-tailed Student *t*-test.

*($P = 0.05$).

Determination of rate constants. Rate constants for the reactions of HNE, acrolein, MVK, and ACR with cysteine sulfhydryl groups were calculated for comparisons with quantum mechanic parameters. Sulfhydryl-containing compounds were incubated with a molar excess of a given type 2 alkene at either pH 7.4 or 8.8, and sulfhydryl concentrations were determined over time by the DTNB method (see above). For each type 2 alkene-sulfhydryl analog combination, the corresponding graph of $\log[SH/SH_0]$ versus time (SH = concentration of sulfhydryl at time t; SH_0 = initial concentration at t_0) was straight (regression analysis; r^2 range = 0.87–0.99), indicating that the reaction followed pseudo first-order kinetics (see example provided in Fig. 4). Pseudo first-order rate constants (k_1) were derived directly from these graphs, and second-order rate constants (k_2) were calculated according to Friedman *et al*. (1965). The rate constant (k) for the reaction of sulfhydryl thiolates with the type 2 alkenes was calculated from the previously described relationship: $\log(k - k_2) = \log k_2 + pK_a - pH$ (Friedman *et al*., 1965; Whitesides *et al*., 1977).

RESULTS

Synaptosomal Function and Free Sulfhydryl Content

Figure 2A shows the *in vitro* effects of graded HNE concentrations on membrane synaptosomal transport. For comparative purposes, the concentration-dependent effects of acrolein, MVK, and ACR are also shown (LoPachin *et al*., 2007a). For each type 2 alkene, parallel measurements of synaptosomal free sulfhydryl contents are also presented (Fig. 2B). Results indicate that exposure of striatal synaptosomes to HNE, acrolein, MVK, or ACR resulted in parallel concentration-dependent reductions in membrane ^{3}H-DA transport (Fig. 2A). As indicated by the relative IC_{50}′s, the potency of HNE was

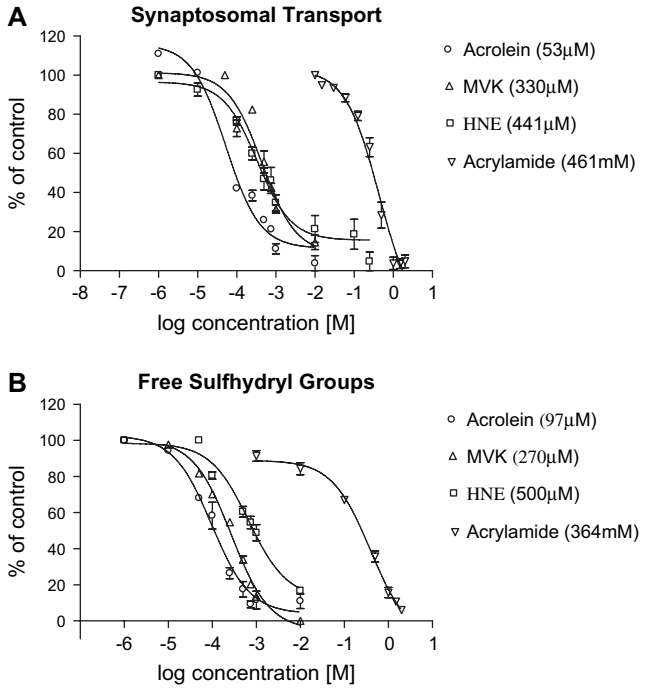

FIG. 2. The concentration-dependent effects of HNE on ^{3}H-DA uptake (A) and free sulfhydryl content (B) in synaptosomes isolated from rat striatum are presented in this figure. For comparative purposes, comparable data for acrolein, MVK, and ACR are shown (LoPachin *et al.*, 2007a). Data are expressed as mean percentage of control ± SEM based on separate experiments (n =3–5). Calculated IC_{50}'s are provided in the parentheses.

comparable to MVK, which were both less potent than acrolein. However, these conjugated alkenes were substantially more potent than ACR. The transport inhibition caused by synaptosomal exposure to these analogs was closely correlated (r^2 = 0.89–0.96) to reductions in free sulfhydryl contents (Fig. 2B). Kinetic analysis of the *in vitro* HNE effect on synaptosomal transport revealed a statistically significant decrease in V_{max}, with no change in K_m (Table 1). In contrast to HNE and the other conjugated α,β-unsaturated carbonyl derivatives, the nonconjugated analogs, allyl alcohol and propanal, did not affect synaptosomal uptake or sulfhydral content (Table 2).

Vesicular Transport

In vitro incubation of synaptic vesicles with HNE produced concentration-dependent decreases in ^{3}H-DA transport (Fig. 3). Similar incubations with acrolein, MVK, or ACR produced parallel decreases in vesicular transport. The order of potency for inhibition of vesicular transport was HNE (56μM) > acrolein (213μM) > MVK (717μM) >> ACR (233mM). Kinetic analysis indicated that HNE significantly decreased the V_{max} of vesicular transport but did not alter corresponding K_m (Table 1). The HNE-induced reductions in V_{max} for synaptosomal (Fig. 2A) and vesicular transports (Fig. 3) are consistent with noncompetitive inhibition due to irreversible (covalent) protein-chemical adduct formation (reviewed in LoPachin and DeCaprio, 2005). The nonconjugated analogs, allyl alcohol and propanal, did not affect vesicular uptake (data not shown).

Softness (σ) and Electrophilic Index (ω) as Determinants of Synaptosomal Toxicity.

Because sulfhydryl groups are soft nucleophiles, the ability of HNE to form a cysteine adduct should be related to the corresponding electrophilic softness of this compound. Electrophilic softness is considered the ease with which electron redistribution takes place during covalent bonding, and thus, the softer the electrophile, the more readily it will form an adduct by accepting outer shell electrons from a soft nucleophile such as the sulfur atom. To determine how electrophilic softness was related to sulfhydryl reactivity, we computed softness (σ) for HNE and selected structural analogs. In addition, we calculated the "electrophilicity index" (ω) for each chemical, which is a higher order quantum mechanical parameter that combines softness with chemical potential and

TABLE 2
Calculated and Experimental Parameters for HNE and the Conjugated and Nonconjugated Analogs

Type 2 alkene	E_{LUMO} (ev)[a]	E_{HOMO} (ev)	σ (ev)	ω (ev)	Log k_2 (pH = 7.4)[b]	Log k[c]	-SH loss (log IC_{50})[d]	Uptake inhibition (log IC_{50})[e]
Acrolein	− 1.70	− 6.98	0.379	3.57	2.596	3.417	− 4.01	− 4.28
MVK	− 1.33	− 6.71	0.372	3.06	2.048	2.953	− 3.57	− 3.48
HNE	− 1.56	− 6.82	0.380	3.29	0.938	1.759	− 3.30	− 3.40
ACR	− 0.69	− 6.77	0.329	2.30	− 1.804	0.767	− 0.44	− 0.36
Allyl alcohol	+0.51	− 6.93	0.269	1.38	—	—	—	—
Propanal	− 0.33	− 6.86	0.307	1.98	—	—	—	—

[a] E_{LUMO} = energy level (ev) of the LUMO; E_{HOMO} = energy level (ev) of the HOMO. The E_{LUMO} and E_{HOMO} values were used to calculate softness (σ) and the electrophilic index (ω) of each electrophile as described in the "Materials and Methods" section.

[b] Second-order reaction rates (k_2) were determined for type 2 alkene reactions with L-cysteine at pH 7.4 (n = 4–6 experiments).

[c] The k_2 values at pH 7.4 were corrected for the corresponding cysteine thiolate concentration according to the algorithm: $\log(k - k_2) = \log k_2 + pK_a - pH$.

[d] Synaptosomal sulfhydryl (–SH) loss was determined in striatal synaptosomes exposed to HNE or other type 2 alkenes (n = 4–6 experiments).

[e] Inhibition of membrane ^{3}H-DA uptake was determined in striatal synaptosomes exposed to HNE or other type 2 alkenes (n = 4–6 experiments).

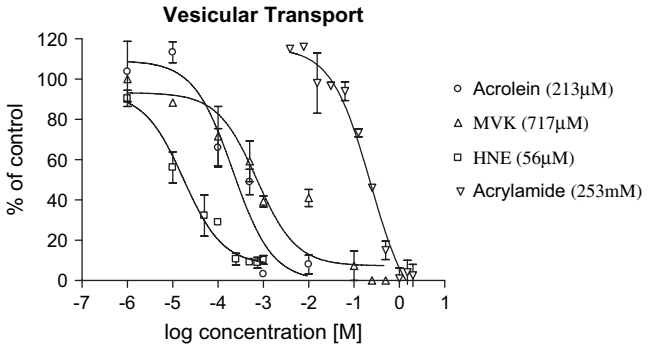

FIG. 3. The concentration-dependent effects of HNE on ^{3}H-DA transport in striatal synaptic vesicles are presented in this figure. For comparative purposes, comparable data for acrolein, MVK, and ACR are shown (LoPachin *et al*., 2007a). Data are expressed as mean percentage of control ± SEM based on separate experiments (n =3–5). Calculated IC_{50}'s are provided in the parentheses.

TABLE 3
Calculated Quantum Mechanical Parameters for Nucleophilic Amino Acids

Amino acid residue[a]	E_{LUMO} (ev)	E_{HOMO} (ev)	μ (ev)	σ (ev)
Cysteine thiolate (− 1)	4.76	− 0.35	2.21	0.391
Cysteine thiol (0)	0.14	− 5.87	− 2.87	0.330
Histidine (0)	0.30	− 5.75	− 2.75	0.331
Lysine (+ 1)	− 2.98	− 10.39	− 6.69	0.270

[a]For each nucleophile, quantum mechanical parameters were calculated based on the predominant ionization state (in parentheses) at pH 7.4. To model a cysteine catalytic triad, quantum mechanical parameters were also calculated for the anionic thiolate state (− 1). E_{LUMO} = energy level (ev) of the LUMO; E_{HOMO} = energy level (ev) of the HOMO. E_{LUMO} and E_{HOMO} values were used to calculate the chemical potential (μ) of the nucleophile and corresponding softness (σ) as described in the ''Materials and Methods'' section.

is, therefore, a descriptor of electrophile reactivity (Chattaraj *et al*., 2006). Based on the corresponding σ values, HNE, acrolein, and MVK are of comparable softness and, collectively, are softer electrophiles than ACR. The respective electrophilic index (ω), however, indicated a rank order of acrolein > HNE > MVK >>ACR (Table 2). The nonconjugated analogs, allyl alcohol and propanal, are not Michael acceptors and therefore had correspondingly lower σ and ω values (Table 2).

To establish the correspondence between these descriptors and sulfhydryl reactivity, we determined the respective second-order rate constants (k_2) for the reactions of HNE and structural analogs with the sulfhydryl group of L-cysteine. Results (Table 2) show that, among the type 2 alkenes tested, the k_2 value for acrolein was largest, reflecting a relatively fast rate of reaction. In contrast, the rate constants for HNE and MVK were intermediate, whereas the corresponding ACR constant was the smallest among the type 2 alkenes, indicating relatively slow kinetics. When the log k_2 values for each chemical were compared by linear regression to the respective σ and ω (Table 2), a reasonable correlation existed ($r^2 > 0.83$ and 0.84, respectively). If sulfhydryl adduct formation is an initiating step in type 2 alkene neurotoxicity, the k_2 rate constants should correspond to the relative ability of these chemicals to produce *in vitro* neurotoxicity. Indeed, our results (Table 2) show that the electrophiles with faster kinetics (HNE, acrolein, and MVK) were the most potent (lowest IC_{50} values) conjugated alkenes with respect to depletion of synaptosomal thiols and impairment of synaptosomal membrane transport. In contrast, ACR which formed sulfhydryl adducts slowly (lower k_2 value) was least potent (higher IC_{50} values). Regression analysis showed that the log k_2 values were highly correlated to the log of the respective IC_{50}'s for synaptosomal uptake inhibition ($r^2 = 0.95$) and sulfhydryl loss ($r^2 = 0.96$). Together, these data suggest that the degree of softness or electrophilicity of the conjugated alkenes is related to the corresponding ability (reaction rate) to form sulfhydryl adducts and to thereby produce synaptosomal toxicity.

Chemical Potential (μ) and the Nucleophilic Index (ω^-) as Predictors of Nucleophilic Targeting

HNE and other type 2 alkenes are soft electrophiles that preferentially form adducts with soft nucleophiles. Reduced cysteine sulfhydryl groups, which exist in either the thiol or the anionic thiolate states, are the principle soft biological nucleophiles. Amino groups on lysine or histidine residues are also nucleophilic and, consequently, are potential sites of HNE adduction. To investigate the relative activities of these different nucleophiles in HNE adduct formation, we calculated the corresponding softness (σ) and chemical potential (μ). This latter parameter indicates the relative ability of a nucleophilic species to transfer electron density to an electrophile. The σ values presented in Table 3 indicate that the thiolate state of the cysteine sulfhydryl group is softer (higher positive value) than the other nucleophiles. Furthermore, the respective μ values demonstrate that the thiolate state is substantially more nucleophilic (more positive μ value) than the cysteine thiol state, the lysine ε-amino group, or the imidazole moiety of histidine. These data demonstrate that the cysteine thiolate state is a better nucleophile than lysine, histidine, or the sulfhydryl thiol state. The molecular orbital energy was also used to calculate the nucleophilicity index (ω^-), which is a recently developed higher order parameter that considers the respective hardness (σ) and chemical potential (μ) of both the electrophilic (type 2 alkene) and nucleophilic (cysteine, histidine, or lysine) reactants (Jaramillo *et al*., 2006). This parameter is, therefore, a measure of the likelihood of subsequent adduct formation. As suggested by the respective ω^- values (Table 4), HNE and the type 2 alkenes preferentially form adducts with cysteine thiolate sites (higher ω^- value) as opposed to histidine, lysine, or thiol residues (lower ω^- values).

TABLE 4
Calculated Nucleophilic Indices (ω^-) for Reactions of HNE and Other Type 2 Alkenes With Possible Nucleophilic Targets

Electrophile[a]	ω^- Cys (− 1)	ω^- Cys (0)	ω^- His (0)	ω^- Lys (− 1)
Acrolein	2.03	0.103	0.123	0.253
HNE	1.93	0.083	0.102	0.287
MVK	1.83	0.064	0.081	0.319
ACR	1.50	0.036	0.048	0.346

[a]For each nucleophile-electrophile pairing, ω^- was calculated based on the predominant ionization state (in parentheses) of the potential amino acid target at pH 7.4. To model a cysteine catalytic triad, ω^- was also calculated for the anionic thiolate state (− 1). The ω^- descriptor is a higher order quantum mechanical parameter that considers the respective hardness and chemical potential of both the electrophilic (e.g., HNE) and nucleophilic (e.g., cysteine) reactants and is, therefore, a measure of adduct formation potential.

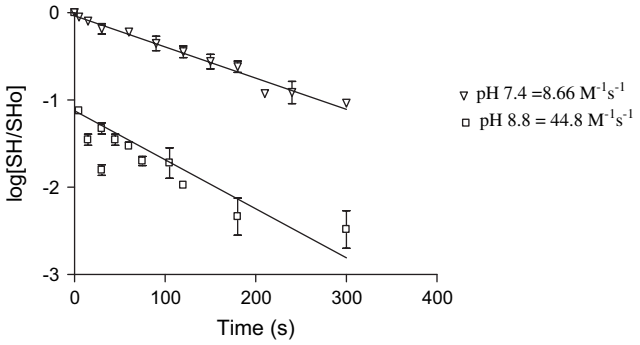

FIG. 4. This figure shows a plot of $\log[SH/SH_0]$ versus time (s) for the reaction of HNE with L-cysteine at pH 7.4 or pH 8.8, where SH_0 = initial sulfhydryl concentration at time zero. The respective second-order rate constants (k_2) for these reactions are provided in the figure.

If, as the calculated nucleophilic descriptors suggest, the thiolate state is the preferred HNE target, this should be reflected in corresponding chemical reaction rates. The thiol-thiolate equilibrium of L-cysteine is a function of pK_a (8.15), and therefore, we measured sulfhydryl loss at pH 7.4 and pH 8.8 (Fig. 4). At pH 8.8, the thiolate concentration will increase relative to that at pH 7.4, and if the thiolate is the preferred adduct target, the respective reaction rate for HNE and L-cysteine will increase in proportion to the enlarging thiolate concentration as determined by the pK_a. Accordingly, results show that at pH 8.8 the reaction of HNE and cysteine is considerably increased relative to pH 7.4 (Fig. 4). Corroborative studies showed that this pH-dependent rate increase occurred for all type 2 alkenes evaluated (data not shown). The k_2 values at a given pH can be corrected for the corresponding thiolate concentrations using the formula: $\log(k - k_2) = \log k_2 + pK_a - pH$. For each α,β-unsaturated carbonyl derivative, the corresponding thiolate rate constants at either pH were similar and were well correlated to μ ($r^2 = 0.96$; Table 3) and ω^- ($r^2 = 0.91$; Table 4).

Application of Quantum Mechanical Descriptors to In Vitro *Neurotoxicity*

As a practical demonstration of nucleophilic targeting, we determined the relative abilities of NAC (cysteine analog), carnosine (histidine analog), and NAL (lysine analog) to scavenge HNE and thereby modify *in vitro* neurotoxicity. Preliminary studies showed that the selected nucleophiles did not affect synaptosomal function at the concentrations used (data not shown). Results (Fig. 5) indicate that NAC significantly reduced HNE neurotoxicity; for example, the IC_{50} for HNE inhibition of synaptosomal uptake (Fig. 5A) was 441μM, which increased to 2.25mM in the presence of NAC. In contrast, neither NAL nor carnosine affected the *in vitro* neurotoxicity of HNE (Fig. 5A). Similarly, in a recent study (LoPachin *et al.*, 2007a), we showed that NAC (500μM), but not NAL (500 μM), decreased the *in vitro* neurotoxicity of acrolein and other type 2 alkenes. We did not, however, assess the protective effects of carnosine. Here we report that carnosine (500μM) also did not affect the *in vitro* neurotoxicity of other type 2 alkenes (Fig. 6). These data are consistent with corresponding quantum mechanical computations since NAL ($\mu = -2.58$) and carnosine ($\mu = -2.17$) are less nucleophilic than NAC ($\mu = 5.97$) and are, therefore, less capable of scavenging HNE and other α,β-unsaturated carbonyl derivatives.

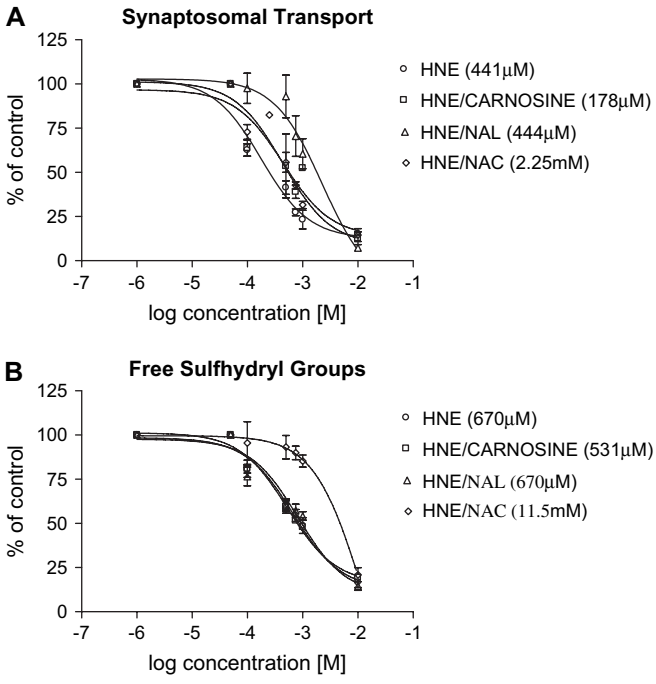

FIG. 5. The effects of NAC, NAL, and carnosine on the inhibition of ^{3}H-DA transport (A) and loss of free sulfhydryl groups (B) in HNE-exposed striatal synaptosomes (n = 4–6 experiments) are presented in this figure. Control data are as follows: synaptosomal transport = 17 ± 2 nmol/mg protein/min; synaptosomal free sulfhydryl content = 132 ± 4 pmol/mg protein. Data are expressed as mean percentage control ± SEM. Calculated IC_{50}'s are provided in the parentheses.

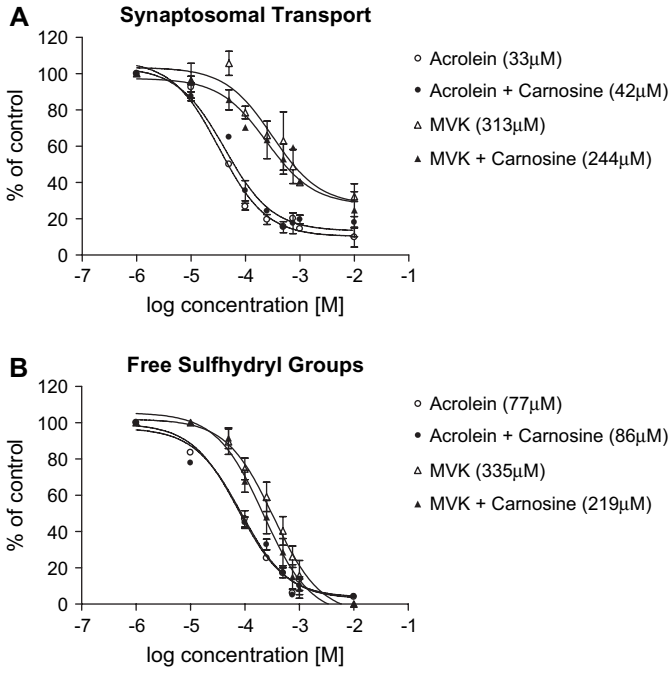

FIG. 6. The effects of carnosine on the inhibition of ^{3}H-DA transport (A) and loss of free sulfhydryl groups (B) in acrolein- or MVK-exposed striatal synaptosomes ($n = 4$–6 experiments) are presented in this figure. Control data are provided in the legend of Figure 5. Data are expressed as mean percentage control ± SEM. Calculated IC_{50}'s are provided in the parentheses.

DISCUSSION

The results of this study show that, like other type 2 alkenes, *in vitro* HNE exposure produced concentration-dependent decreases in the ^{3}H-DA membrane transport and vesicular storage of striatal synaptosomes (see also Castegna *et al.*, 2004; Keller *et al.*, 1997a,b; Pocernich *et al.*, 2001; Subramaniam *et al.*, 1997). These neurotoxic effects were closely correlated to graded decreases in synaptosomal free sulfhydryl content. The respective IC_{50}'s are comparable to data from previous *in vitro* neurotoxicity studies (Morel *et al.*, 1999) and are consistent with intracellular HNE concentrations that occur during cell injury (Dalle-Donne *et al.*, 2007; Poli and Schaur, 2000). Relative to other type 2 alkenes, HNE was comparable to MVK, whereas both were significantly less potent (lower IC_{50}'s) than acrolein (Figs 2 and 3). ACR was the weakest neurotoxicant tested in this synaptosomal model. The respective neurotoxic potencies indicated a rank order (i.e., acrolein > MVK ≥HNE >> ACR) that corresponded ($r^2 =$ 0.90–0.96) to the respective second-order rate constants (log k_2) and quantum mechanical parameters, σ and ω. These results support prior studies (LoPachin *et al.*, 2007a), which demonstrated that α,β-unsaturated aldehydes and ketones such as acrolein and MVK were more reactive and more potent synaptotoxicants than amide and ester derivatives such as ACR and methyl acrylate, respectively. These relative differences in synaptotoxicity are directly related to corresponding differences in electrophilic reactivity. As the respective quantum mechanical parameters indicate (Table 2), ACR is a weaker electrophile that slowly forms Michael-type adducts with soft nucleophilic sulfhydryl groups on cysteine residues, whereas HNE is a stronger (softer) electrophile that rapidly forms such adducts (Friedman *et al.*, 1965; LoPachin *et al.*, 2007a,b). Thus, within the short incubation time of this study (15 min), higher ACR concentrations must be used to achieve the previously determined minimal synaptosomal adduct concentration (0.50 ng cysteine adduct/μg protein; see Barber and LoPachin, 2004) needed to cause toxicity (compare respective IC_{50}′s in Fig. 2). Whereas differences in potency exist, it is important to note that corresponding neurotoxic efficacies (maximal effects) among the tested type 2 alkenes are equivalent (Fig. 2). This means that, despite their slow rate of formation, ACR adducts have the same neurotoxicological impact as the more rapidly forming HNE or acrolein adducts.

Predictably, HNE, an α,β-unsaturated aldehyde, possessed considerable *in vitro* neurotoxic potency and exhibited a relatively fast reaction rate. However, within the aldehyde/ketone subgroup, there existed significant differences in correlation among the quantum mechanical, kinetic, and neurochemical parameters. Specifically, the rate constants (log k_2) for this subgroup were well correlated to the respective *in vitro* IC_{50}′s, although these kinetic data were less correlated to ω and poorly correlated to σ (Table 2). The lack of correspondence among this subgroup is attributable to HNE and the consequential slowing of the adduct reaction due to steric hindrance imposed by the alkane tail (Friedman and Wall, 1966). Since neither σ nor ω account for steric factors, such disagreement among the aldehyde/ketone type 2 alkenes is expected.

Growing evidence suggests that the molecular neurotoxic mechanism of HNE and other type 2 alkenes involves a two-step process: that is, initial adduction of protein nucleophiles and subsequent loss of function (reviewed in LoPachin *et al.*, 2008a). Our structure-toxicity analyses (the present study, LoPachin *et al.*, 2007a) indicate that the nucleophilic target of the type 2 alkenes is determined by the α,β-unsaturated carbonyl structure of these chemicals. This structure is a conjugated system, characterized by mobile *pi* electrons and, because the carbonyl oxygen atom is electron withdrawing, a localized area of electron deficiency develops at the β carbon of HNE. The α,β-unsaturated carbonyl structure is, therefore, a soft electrophile according to the hard and soft acids and bases theory (Pearson, 1990). Electrophile-nucleophile interactions are not absolute but rather occur along a continuum of relative reactivity according to the principal of "like reacts with like" (reviewed in LoPachin and DeCaprio, 2005; LoPachin *et al.*, 2008a). Thus, as a soft electrophile, HNE will preferentially form adducts with comparably soft nucleophiles. The softness of a nucleophile is determined by the polarizability of corresponding valence electrons. Sulfur, as opposed to nitrogen or oxygen atoms, has a large atomic radius

with highly polarizable valence electrons and is, by definition, the softest nucleophile in biological systems.

Biological free sulfhydryl groups can exist in the thiol state (-SH) or in the anionic thiolate state ($-S^-$). Calculations of corresponding softness (σ) and chemical potential (μ) indicate that, relative to sulfhydryl thiols, the thiolate state is significantly more nucleophilic (Table 3) and is, consequently, the preferential target of HNE. The close correspondence of the neurotoxic potencies (IC_{50}'s; Table 2; see also Fig. 4) to the second-order rate constants (k_2) corrected for the actual thiolate concentration (k) provides direct kinetic evidence for thiolate targeting by HNE and the type 2 alkenes (LoPachin *et al*., 2007b). The pK_a of the sulfhydryl side chain is 8.5, and therefore, the anion concentration should be low ($\leq$ 10%) at pH 7.4. However, the thiolate state is more prevalent than predicted due to the existence of low pK_a cysteine sulfhydryl groups within highly specialized amino acid sequences known as catalytic triads (reviewed in LoPachin and Barber, 2006; Stamler *et al*., 1997, 2001). Proton shuttling between flanking or proximal ($\leq$ 6Å) basic amino acid residues (histidine, arginine, lysine) and their acidic counterparts (aspartate, glutamate) can deprotonate the sulfhydryl group and, thereby, lower the corresponding pK_a by several units (e.g., see Britto *et al*., 2002; Sfakianos *et al*., 2002). Adduct formation between HNE and sulfhydryl thiolate groups occurs via a 1,4-Michael-type addition reaction, that is, nucleophilic attack at the β-carbon with subsequent addition across the carbon-carbon double bond. The resulting intermediate product, a saturated aldehyde, then undergoes an intramolecular reaction with the hydroxyl group to form a cyclic hemiacetal, which is the predominant adduct form (reviewed in Esterbauer *et al*., 1991; Petersen and Doorn, 2004; Witz, 1989). That HNE and the type 2 alkenes preferentially form stable 1,4-adducts with cysteine sulfhydryl groups has been demonstrated by the isolation of these adducts and subsequent quantitation using mass spectrometry and other proteomic approaches (Aldini *et al*., 2005; Barber and LoPachin, 2004; Dalle-Donne *et al*., 2007; Doorn and Petersen, 2002, 2003; Ishii *et al*., 2003; LoPachin *et al*., 2006, 2007a; Uchida and Stadtman, 1993a; Uchida *et al*., 1998a; van Iersel *et al*., 1997; also see early studies by Friedman and Wall, 1966; Friedman *et al*., 1965).

Amino groups on lysine or histidine residues are also nucleophiles and are, therefore, potential sites for HNE adduction via 1,4-Michael-type reactions. However, the imidazole moiety of histidine and the ε-amino group of lysine are significantly harder nucleophiles than the relatively soft thiolate state of cysteine, that is, compare respective σ and μ data in Table 3. Consequently, these harder nucleophiles are kinetically unfavorable targets for HNE and other soft electrophiles (reviewed in Hinson and Roberts, 1992; Esterbauer *et al*., 1991; LoPachin and DeCaprio, 2005; LoPachin *et al*., 2008a). Furthermore, at physiological pH (7.4), the secondary amine of histidine is mostly deprotonated based on a corresponding pK_a of 6.0. As reflected in the μ and ω^- values (Tables 3 and 4), the nucleophilicity of this neutral state (0) is substantially lower than that of the sulfhydryl anionic state ($-$ 1). Also at physiological pH, the primary amine side chain of lysine (pK_a = 10.5) is protonated (+ 1) and is, as the respective μ and ω^- values indicate (Tables 3 and 4), a very poor nucleophile. These electronic characteristics do not, however, mean that HNE is incapable of forming Lys or His adducts (e.g., see Bruenner *et al*., 1995; Nadkarni and Sayre, 1995; Uchida and Stadtman, 1993b), rather the kinetics of adduct formation are extremely slow. Determinations of second-order rate constants (mean k_2 ± SD $M^{\wedge}(-1)s^{\wedge}(-1)$ showed that Cys (1.33 ± 0.083) was significantly more reactive toward HNE than His (2.14 ± 0.312×10^{-3}) or Lys ($1.33 \pm 0.050 \times 10^{-3}$; Doorn and Petersen, 2002, 2003; see also Lin *et al*., 2005; van Iersel *et al*., 1997).

As an alternative to 1,4-Michael addition, the carbonyl carbon atom of HNE could form adducts with primary amines (e.g., Lys) via a 1,2-addition. Nadkarni and Sayre (1995) have provided indirect evidence that HNE forms such adducts with primary amines and that subsequent Schiff base formation is prevalent in solvent-isolated (buried) hydrophobic protein microenvironments. However, the corresponding kinetics are inherently slow, and the Schiff base product is reversible (reviewed in Petersen and Doorn, 2004). That this reaction might not be neurotoxicologically relevant is suggested by recent *in vitro* studies, which showed that graded exposure of striatal synaptosomes to propanal (an aldehyde) did not affect neurotransmitter release, reuptake, or vesicular storage (Table 2; see also LoPachin *et al*., 2007a). If, as the preceding data imply, soft-soft interactions govern the adduct kinetics of HNE and other type 2 alkenes, then a soft nucleophilic cysteine analog (NAC) should modify the development of *in vitro* synaptosomal toxicity by rapidly scavenging HNE. In contrast, neurotoxicity should not be influenced by incubation with harder lysine (NAL) or histidine (carnosine) analogs that react more slowly with HNE and are, therefore, slower scavengers. Corroborative studies (Figs 5 and 6) showed that NAC significantly retarded the development of synaptosomal dysfunction induced by HNE and other type 2 alkenes, whereas neither NAL nor carnosine were effective.

Our findings thus far indicate that HNE and the type 2 alkenes preferentially and rapidly form Michael-type adducts with sulfhydryl groups. This is in contrast to Lys or His adduction, which is kinetically unfavored and, therefore, slower. However, the rate of amino acid adduct formation does not determine which residue is the toxicologically significant target. Instead, it is the role of that residue in protein structure or function and the disruptive consequences of adduction that determine significance. Thus, although HNE adducts of Lys and His residues are associated with several chronic neuropathological states (Montine *et al*., 2002; Uchida, 2003) and can be isolated from certain *in vitro* conditions (Nadkarni and Sayre, 1995; Uchida and Stadtman, 1993b), the toxicological relevance of these adducts has not been established. In contrast, anionic thiolates within cysteine catalytic

triads are found in the active sites of many proteins (e.g., vacuolar ATPase, NSF) that participate in critical presynaptic processes such as neurotransmitter storage and release (reviewed in Barford, 2004; LoPachin and Barber, 2006; LoPachin *et al*., 2008a; Stamler *et al*., 2001). Not only are these catalytic thiolates targets for the type 2 alkenes, they are also acceptors for endogenous nitric oxide (NO; Forman *et al*., 2004; Stamler *et al*., 2001). NO is a biological electrophile that reversibly forms adducts with thiolate groups and thereby modulates cellular processes by transiently regulating the activities of proteins (Esplugues, 2002; Kiss, 2000; LoPachin and Barber, 2006). We have recently demonstrated that the type 2 alkenes inhibit neurotransmitter release by forming adducts with Cys 264 of NSF. This cysteine is located within a catalytic triad that regulates the rate-limiting ATPase function of NSF in the synaptic vesicle cycle (Barber and LoPachin, 2004; Barber *et al*., 2007; LoPachin *et al*., 2007a). Thus, irreversible adduction of essential NO-targeted thiolates by HNE and the type 2 alkenes has toxicological significance.

How does thiolate adduction relate to *in vivo* mechanisms of type 2 alkene toxicity? HNE and acrolein are by-products of lipid peroxidation that develops secondary to cellular oxidative stress. A growing body of evidence suggests that neurodegenerative conditions such as AD are characterized by early neuronal oxidative damage and nerve terminal dysfunction. Although the mechanism of AD synaptotoxicity has not been determined, numerous studies have reported elevated levels of HNE, acrolein, and their respective protein adducts in relevant brain regions (e.g., amygdala, hippocampus) of AD patients and transgenic animal models (reviewed in LoPachin *et al*., 2008a,b). Our data, therefore, offer a causal connection between regional synaptic impairment and the endogenous liberation of type 2 alkenes in the neurodegenerative brain; that is, acrolein and HNE form irreversible adducts with NO thiolate acceptors on presynaptic proteins, the resulting loss of NO neuromodulation disrupts neurotransmission, and promotes memory and cognitive deficits. Nerve terminals, due to the exceptionally slow turnover rates of many resident proteins, are selectively vulnerable to damage by low-level exposure to electrophiles. Slower protein turnover promotes adduct accumulation and progressive (cumulative) impairment of presynaptic processes (reviewed in LoPachin and Barber, 2006; LoPachin *et al*., 2008a,b). However, our studies (LoPachin *et al*., 2007a,b) suggest that chemicals in the type 2 alkene class share a common ability to cause synaptotoxicity through adduction of sulfhydryl thiolate groups. Whereas neurotoxicity is a well-documented outcome of *in vivo* ACR intoxication, peripheral exposure (e.g., oral) to acrolein or MVK is associated with systemic toxicity. As we have recently discussed (LoPachin *et al*., 2008a), this apparent toxicological conundrum is due to relative differences in electrophilic reactivity. Thus, acrolein and MVK are highly electrophilic and rapidly form adducts with sulfhydryl groups. Following systemic intoxication, this rapid adduct formation essentially limits tissue distribution of these reactive type 2 alkenes. As a result, the peripheral site of absorption determines the corresponding toxic manifestations, which are also mediated by a thiolate-based mechanism (see references in LoPachin *et al*., 2008a). As a weak water-soluble electrophile, ACR is less susceptible to the limiting influence of systemic "adduct buffering" and has a correspondingly larger volume of distribution that encompasses central nervous system nerve terminals. Because synaptotoxicity is a type 2 alkene characteristic, exposure to ACR and other weak electrophilic derivatives (e.g., acrylonitrile, methyl acrylate), for example, through environmental pollution or food contamination, might accelerate the endogenous neurodegenerative cascade of HNE/acrolein production and subsequent nerve terminal damage (reviewed in LoPachin *et al*., 2008a,b).

FUNDING

National Institutes of Health grant from the National Institute of Environmental Health Sciences (RO1 ES03830-21).

REFERENCES

Aldini, G., Dalle-Donne, I., Vistoli, G., Facino, R. M., and Carini, M. (2005). Covalent modification of actin by 4-hydroxy-trans-2-nonenal (HNE): LC-ESI-MS/MS evidence for Cys374 Michael adduction. *J. Mass Spectrom.* **40,** 946–954.

Barber, D. S., Stevens, S., and LoPachin, R. M. (2007). Proteomic analysis of rat striatal synaptosomes during acrylamide intoxication at a low dose rate. *Toxicol. Sci.* **100,** 156–167.

Barber, D. S., and LoPachin, R. M. (2004). Proteomic analysis of acrylamide-protein adduct formation in rat brain synaptosomes. *Toxicol. Appl. Pharmacol.* **201,** 120–136.

Barford, D. (2004). The role of cysteine residues as redox-sensitive regulatory switches. *Curr. Opin. Struct. Biol.* **14,** 679–686.

Britto, P. J., Knipling, L., and Wolff, J. (2002). The local electrostatic environment determines cysteine reactivity of tubulin. *J. Biol. Chem.* **277,** 29018–29027.

Bruenner, B. A., Jones, A. D., and German, J. B. (1995). Direct characterization of protein adducts of the lipid peroxidation product 4-hydroxy-2-nonenal using electrospray mass spectrometry. *Chem. Res. Toxicol.* **8,** 552–559.

Castegna, A., Lauderback, C. M., Mohmmad-Abdul, H., and Butterfield, D. A. (2004). Modulation of phospholipid asymmetry in synaptosomal membranes by the lipid peroxidation products, 4-hydroxynonenal and acrolein: Implications for Alzheimer's disease. *Brain Res.* **1004,** 193–197.

Chattaraj, P. K. (2001). Chemical reactivity and selectivity: Local HSAB principal versus frontier orbital theory. *J. Phys. Chem. A* **105,** 511–513.

Chattaraj, P. K., Sarkar, U., and Roy, D. R. (2006). Electrophilicity index. *Chem. Rev.* **106,** 2065–2091.

Dalle-Donne, I., Vistoli, G., Gamberoni, L., Giustarini, D., Colmbo, R., Facino, R. M., Rossi, R., Milzani, A., and Aldini, G. (2007). Actin Cys374 as a nucleophilic target of α,β-unsaturated aldehydes. *Free Radic. Biol. Med.* **42,** 583–598.

Doorn, J. A., and Petersen, D. R. (2002). Covalent modification of amino acid nucleophiles by the lipid peroxidation products 4-hydroxy-2-nonenal and 4-oxo-2-nonenal. *Chem. Res. Toxicol.* **15,** 1445–1450.

Doorn, J. A., and Petersen, D. R. (2003). Covalent adduction of nucleophilic amino acids by 4-hydroxynonenal and 4-oxononenal. *Chem. Biol. Interact.* **143–144,** 93–100.

Esplugues, J. V. (2002). NO as a signaling molecule in the nervous system. *Br. J. Pharmacol.* **135,** 1079–1095.

Esterbauer, H., Schaur, R. J., and Zollner, H. (1991). Chemistry and biochemistry of 4-hydroxynonenal, malonaldehyde and related aldehydes. *Free Radic. Biol. Med.* **11,** 81–128.

Forman, H. J., Fukuto, J. M., and Torres, M. (2004). Redox signaling: Thiol chemistry defines which reactive oxygen and nitrogen species can act as second messengers. *Am. J. Physiol. Cell Physiol.* **287,** C246–C256.

Friedman, M., Cavins, J. F., and Wall, J. S. (1965). Relative nucleophilic reactivities of amino groups and mercaptide ions in addition reactions with α,β-unsaturated compounds. *J. Am. Chem. Soc.* **87,** 3672–3682.

Friedman, M., and Wall, J. S. (1966). Additive linear free-energy relationships in reaction kinetics of amino groups with α,β-unsaturated compounds. *J. Org. Chem.* **31,** 2888–2894.

Halliwell, B. (2006). Oxidative stress and neurodegeneration: Where are now? *J. Neurochem.* **97,** 1634–1658.

Hinson, J. A., and Roberts, D. W. (1992). Role of covalent and noncovalent interactions in cell toxicity: Effects on proteins. *Ann. Rev. Pharmacol. Toxicol.* **32,** 471–510.

Ishii, T., Tatsuda, E., Kumazawa, S., Nakayama, T., and Uchida, K. (2003). Molecular basis of enzyme inactivation by an endogenous electrophile 4-hydroxy-2-nonenal: Identification of modification sites in glyceraldehyde-3-phosphate dehydrogenase. *Biochemistry* **42,** 3473–3480.

Jaramillo, P., Periz, P., Contreras, R., Tiznada, W., and Fuentealba, P. (2006). Definition of a nucleophilicity scale. *J. Phys. Chem.* **110,** 8181–8187.

Jenner, P. (2003). Oxidative stress in Parkinson's disease. *Ann. Neurol.* **53,** S26–S38.

Keller, J. N., Mark, R. K., Bruce, A. J., Blanc, E., Rothstein, J. D., Uchida, K., Waeg, G., and Mattson, M. P. (1997a). 4-Hydroxynonenal, an aldehyde product of membrane lipid peroxidation, impairs glutamate transport and mitochondrial function in synaptosomes. *Neuroscience* **80,** 685–696.

Keller, J. N., Pang, Z., Geddes, J. W., Begley, J. G., Germeyer, A., Waeg, G., and Mattson, M. P. (1997b). Impairment of glucose and glutamate transport and induction of mitochondrial oxidative stress and dysfunction in synaptosomes by amyloid β-peptide: Role of the lipid peroxidation product 4-hydroxynonenal. *J. Neurochem.* **69,** 273–284.

Kemp, D. S., and Vellaccio, F. (1980). Carbonyl condensation reactions. In *Organic Chemistry,* Chap. 24, pp. 839–874. Worth Publishers, New York.

Kiss, J. P. (2000). *Role of nitric oxide in the regulation of monoaminergic neurotransmission.* **52,** 459–466.

Lin, D., Lee, H., Liu, Q., Perry, G., Smith, M. A., and Sayre, L. M. (2005). 4-Oxy-2-nonenal is both more neurotoxic and more protein reactive than 4-hydroxy-2-nonenal. *Chem. Res. Toxicol.* **18,** 1219–1231.

Lipton, S. A., Choi, Y.-B., Takahasi, H., Zhang, D., Godzik, A., and Bankston, L. A. (2002). Cysteine regulation of protein function—as exemplified by NMDA-receptor modulation. *Trends Neurosci.* **25,** 474–480.

LoPachin, R. M., and Barber, D. S. (2006). Synaptic cysteine sulfhydryl groups as targets of electrophilic neurotoxicants. *Toxicol. Sci.* **94,** 240–255.

LoPachin, R. M., Barber, D. S., and Gavin, T. (2008a). Molecular mechanisms of the conjugated α,β-unsaturated carbonyl derivatives: Relevance to neurotoxicity and neurodegenerative diseases. *Toxicol. Sci.* **104,** 235–249.

LoPachin, R. M., Barber, D. S., Geohagen, B. C., Gavin, T., He, D., and Das, S. (2007a). Structure-toxicity analysis of type-2 alkenes: In vitro neurotoxicity. *Toxicol. Sci.* **95,** 136–146.

LoPachin, R. M., Barber, D. S., He, D., and Das, S. (2006). Acrylamide inhibits dopamine uptake in rat striatal synaptic vesicles. *Toxicol. Sci.* **89,** 224–234.

LoPachin, R. M., and DeCaprio, A. P. (2005). Protein adduct formation as a molecular mechanism in neurotoxicity. *Toxicol. Sci.* **86,** 214–225.

LoPachin, R. M., Gavin, T., and Barber, D. S. (2008b). Type-2 alkenes mediate synaptotoxicity in neurodegenerative diseases. *Neurotoxicology* **29,** 871–882.

LoPachin, R. M., Gavin, T., Geohagen, B. C., and Das, S. (2007b). Neurotoxic mechanisms of electrophilic type-2 alkenes: Soft-soft interactions described by quantum mechanical parameters. *Toxicol. Sci.* **98,** 561–570.

LoPachin, R. M., Schwarcz, A. I., Gaughan, C. L., Mansukhani, S., and Das, S. (2004). In vivo and in vitro effects of acrylamide on synaptosomal neurotransmitter uptake and release. *Neurotoxicology* **25,** 349–363.

Lovell, M. A., Xie, C., and Markesbery, W. R. (2000). Acrolein, a product of lipid peroxidation, inhibits glucose and glutamate uptake in primary neuronal cultures. *Free Radic. Biol. Med.* **29,** 714–720.

Lovell, M. A., Xie, C., and Markesbery, W. R. (2001). Acrolein is increased in Alzheimer's disease brain and is toxic to primary hippocampal cultures. *Neurobiol. Aging* **22,** 187–194.

Mattson, M. P. (2004). Pathways towards and away from Alzheimer's disease. *Nature* **430,** 631–639.

Maynard, A. T., Huang, M., Rice, W. G., and Covell, D. G. (1998). Reactivity of the HIV-1 nucleocapsid protein p7 zinc finger domains from the perspective of density-functional theory. *Proc. Natl. Acad. Sci. U.S.A.* **95,** 11578–11583.

Montine, T. J., Neeley, M. D., Quinn, J. F., Beal, M. F., Markesbery, W. S., Roberts, L. J., II., and Morrow, J. D. (2002). Lipid peroxidation in aging brain and Alzheimer's disease. *Free Radic. Biol. Med.* **33,** 620–626.

Morel, P., Tallineau, C., Pontcharraud, R., Piriou, A., and Huguet, F. (1999). Effects of 4-hydroxynonenal, a lipid peroxidation product, on dopamine transport and Na/K ATPase in rat striatal synaptosomes. *Neurochem. Int.* **33,** 531–540.

Nadkarni, D. V., and Sayre, L. M. (1995). Structural definition of early lysine and histidine adduction chemistry of 4-hydroxynonenal. *Chem. Res. Toxicol.* **8,** 284–291.

Pearson, R. G. (1990). Hard and soft acids and bases—The evolution of a chemical concept. *Coord. Chem. Rev.* **100,** 403–425.

Petersen, D. R., and Doorn, J. A. (2004). Reactions of 4-hydroxynonenal with proteins and cellular targets. *Free Radic. Biol. Med.* **37,** 937–945.

Pocernich, C. B., Cardin, A. L., Racine, C. L., Lauderback, C. M., and Butterfield, D. A. (2001). Glutathione elevation and its protective role in acrolein-induced protein damage in synaptosomal membranes: Relevance to brain lipid peroxidation in neurodegenerative disease. *Neurochem. Int.* **39,** 141–149.

Poli, G., and Schaur, R. J. (2000). 4-Hydroxynonenal in the pathomechanisms of oxidative stress. *IUBMB life* **50,** 315–321.

Sayre, L. M., Smith, M. A., and Perry, G. (2001). Chemistry and biochemistry of oxidative stress in neurodegenerative disease. *Curr. Med. Chem.* **8,** 721–738.

Schultz, T. W., Netzeva, T. I., Roberts, D. W., and Cronin, M. T. D. (2002). Structure-toxicity relationships for the effects to tetrahymena pyriformis of aliphatic carbonyl-containing alpha, beta-unsaturated chemicals. *Chem. Res. Toxicol.* **18,** 330–341.

Sfakianos, M. K., Wilson, L., Sakalian, M., Falany, C. N., and Barnes, S. (2002). Conserved residues in the putative catalytic triad of human bile acid coenzyme A: Amino acid *N*-acetyltransferase. *J. Biol. Chem.* **277,** 47270–47275.

Stamler, J. S., Lamas, S., and Fang, F. C. (2001). Nitrosylation: The prototypic redox-based signaling mechanism. *Cell* **106,** 675–683.

Stamler, J. S., Toone, E. J., Lipton, S. A., and Sucher, N. J. (1997). (S)NO signals: Translocation, regulation and a consensus motif. *Neuron* **18,** 691–696.

Subramaniam, R., Roediger, F., Jordan, B., Mattson, M. P., Keller, J. N., Waeg, G., and Butterfield, A. D. (1997). The lipid peroxidation product, 4-hydroxy-2-*trans*-nonenal, alters the conformation of cortical synaptosomal membrane proteins. *J. Neurochem.* **69,** 1161–1169.

Uchida, K. (2003). 4-Hydroxy-2-nonenal: A product and mediator of oxidative stress. *Prog. Lipid Res.* **42,** 318–343.

Uchida, K., Kanematsu, M., Sakai, K., Matsuda, T., Hattori, N., Mizuno, Y., Suzuki, D., Miyata, T., Noguchi, N., Niki, E., *et al*. (1998a). Protein-bound acrolein: Potential markers for oxidative stress. *Proc. Natl. Acad. Sci. U.S.A.* **95,** 4882–4887.

Uchida, K., and Stadtman, E. R. (1993a). Covalent attachment of 4-hydroxynonenal to glyceraldehyde-3-phosphate dehydrogenase. *J. Biol. Chem.* **268,** 6388–6393.

Uchida, K., and Stadtman, E. R. (1993b). Modification of histidine residues in proteins by reaction with 4-hydroxynonenal. *Proc. Natl. Acad. Sci. U.S.A.* **89,** 4544–4548.

van Iersel, M. L. P. S., Ploemen, J.-P. H. T. M., LoBello, M., Federici, G., and van Bladeren, P. J. (1997). Interactions of α,β-unsaturated aldehydes and ketones with human glutathione S-transferase P1-1. *Chemico Biol. Interact.* **108,** 67–78.

Whitesides, G. M., Lilburn, J. E., and Szajewski, R. P. (1977). Rate of thiol-disulfide interchange reactions between mono- and dithiols and Ellman's reagent. *J. Org. Chem.* **42,** 332–338.

Witz, G. (1989). Biological interactions of α,β-unsaturated aldehydes. *Free Radic. Biol. Med.* **7,** 333–349.

Zarkovic, K. (2003). 4-Hdroxynonenal and neurodegenerative diseases. *Mol. Aspects Med.* **24,** 293–303.